



---

# Microscopic Examination of Crack Growth in a Pressure Vessel Steel

Måns Isacsson  
Torbjörn Narström

Januari 1997

ISSN 1104-1374  
ISRN SKI-R--97/1--SE

---

**SKI**

STATENS KÄRNKRAFTINSPEKTION  
Swedish Nuclear Power Inspectorate

29 - 24

R

SKI Report 97:1

# **Microscopic Examination of Crack Growth in a Pressure Vessel Steel**

Måns Isacson  
Torbjörn Narström

Kungliga Tekniska Högskolan, SE-100 44 Stockholm, Sweden

Januari 1997

SKI Project Number 93261

This report concerns a study which has been conducted for the Swedish Nuclear Power Inspectorate (SKI). The conclusions and viewpoints presented in the report are those of the authors and do not necessarily coincide with those of the SKI.

Norstedts Tryckeri AB  
Stockholm 1998

## **Bakgrund**

För analys av tillväxt hos sprickor kan användas kontinuummekaniska makroskopiska parametrar såsom spänningsintensitetsfaktor  $K$ ,  $J$ -integral  $J$  och spricköppning, CTOD. Vid olika temperaturer relaterat till materialets s.k. omslagstemperatur kan tillväxtmekanismerna på mikroskopisk nivå vara helt olika. Vid låga temperaturer kan ett snabbt, instabilt brott inträffa, medan vid höga temperaturer materialen är sega och spricktillväxten stabil. I ett temperaturområde mellan dessa båda, transitionsområdet, sker spricktillväxt ofta först stabilt, varefter en instabil tillväxt plötsligt inträder.

## **SKI syfte**

Syftet med forskningsprojektet är att vinna bättre förståelse för under vilka betingelser övergången från segt och stabilt till sprött och instabilt brott inträffar.

## **Resultat**

Denna rapport beskriver en mikroskopisk undersökning av materialet A508B hos provstavar med sprickor som belastats till olika nivåer. I mikroskop kunde två duktila tillväxtmekanismer identifieras nämligen tillväxt av hål och lokala skjuvband. Däremot var det svårt att identifiera varifrån det spröda, instabila brottet initierats.

## **Fortsatt verksamhet**

Denna rapport ingår som en del i ett större forskningsprojekt.

Forskningsprojektets namn: Micromechanically based characterization of fracture processes of pressure vessel steels in the transition region.

Utförs av: Kungliga Tekniska Högskolan, institutionerna för Hållfasthetslära och Metallografi.

SKI-projekt nr 93261.

SKI handläggare är Gert Hedner.

## Contents

<b>Summary .....</b>	<b>2</b>
<b>Sammanfattning .....</b>	<b>2</b>
<b>Introduction .....</b>	<b>3</b>
<b>Material .....</b>	<b>5</b>
<b>Fracture mechanics testing .....</b>	<b>12</b>
Specimen description .....	12
Transition curve determination .....	12
Three point bend tests with predetermined load levels.....	13
<b>Microscopic examination.....</b>	<b>14</b>
Technical description of microscopic examination.....	14
Results from the microscopic examination of the ductile crack growth .....	14
Discussion of the ductile crack growth and its micromechanisms .....	19
Results from the microscopic examination of the ductile to brittle region .....	21
<b>Conclusions .....</b>	<b>21</b>
<b>References .....</b>	<b>22</b>

## Summary

A fairly systematic microscopic study concerning ductile and ductile-brittle crack growth in the A508B pressure vessel steel has been performed. The main method of investigation was to subject fracture mechanics specimens (sub-sized three point bend specimens) to predetermined load levels corresponding to different amounts of ductile crack extension. The specimens were then cut perpendicularly to the plane of the crack and the area in front of the crack was examined in a SEM. The object of these examinations was to determine if newly encountered computational results could be correlated to crack extension characteristics and to study whether the mechanism of ductile growth was of the void growth type or of the fast shear mechanism. This is important for further numerical modelling of the process. Both the original material and a specially heat treated piece were investigated. The heat treatment was performed in order to raise the transition temperature to about 60° C with the object to provide a more convenient testing situation. Charpy V tests were performed for the specially heat treated material to obtain the temperature dependence of the toughness. This was also studied by performing fracture toughness determination on the same type of specimens as were used for the microscopic study. The heat treatment used fulfilled the above purpose and the microscopic studies provide a good understanding of the micromechanisms operating in the ductile fracture process for this material.

## Sammanfattning

En relativt systematisk mikroskopstudie av duktil och duktil-spröd spricktillväxt har genomförts för tryckkärlsstålet A508B. Den huvudsakliga metoden för undersökning har varit att belasta brottmekaniska provstavar (mini trepunktsböjprovstavar) till förbestämda lastnivåer som svarar mot olika grader av spricktillväxt. Provstavarna snittades sedan vinkelrätt mot sprickplanet och ytan framför sprickfronten studerades i SEM. Syftet med dessa studier var att utröna om nyligen funna rön från numeriska analyser kunde korreleras till sprickutbrdningskaraktistika och avgöra om den duktila tillväxtmekanismen var av håltillväxttyp eller s.k. snabb skjuvning. Detta är av betydelse för den framtida numeriska modelleringen av processen. Både det virgina materialet och en värmebehandlad variant studerades. Värmebehandlingen företogs för att öka omslagstemperaturen till omkring 60° C för att den experimentella verksamheten skulle underlättas. Charpy V provning genomfördes för att erhålla temperaturberoendet hos segheten. Detta studerades också genom att genomföra brottmekanisk provning på samma typ av provstavar som användes för mikroskopiundersökningen. Värmebehandlingen visade sig ha den önskade effekten och de mikroskopiska undersökningarna medför en god förståelse för de mikromekanismer som förekommer vid duktil spricktillväxt i detta material.

## Introduction

The current development of non-linear fracture mechanics has progressively turned towards bridging of microscopic and macroscopic aspects on crack growth. As the continuum mechanics modelling has sharpened the focus towards smaller length scales, it has become increasingly evident that a proper understanding of the micro mechanisms of crack growth initiation and propagation is necessary. An area where this need is especially pronounced is the description of the ductile to brittle transition in structural steels. The fracture toughness of such a steel is very temperature dependent. For low temperatures, on the lower shelf, where cleavage fracture occurs, rather good theories exist to predict cleavage fracture. One group of such theories is deterministically based, for instance the model of Ritchie, Knott and Rice (1973) and further developments by others. Here the essential assumption is that cleavage fracture occurs when the maximum tensile stress ahead of the crack tip exceeds a critical level over a structurally significant distance. Another group of theories are the weakest link models (cf. Wallin *et al.*, 1984, Wallin, 1989a, b, c, and others). Both these groups of theories result in a one parameter description of the crack tip conditions on the lower shelf since yielding is here mostly insignificant.

For temperatures above the lower shelf, the ductile to brittle transition region, experiments show that significant plastic deformation and sometimes also ductile tearing often precedes cleavage fracture (Wallin, 1989c). In recent years an extensive amount of work has been done to derive mathematical models and numerical tools that can predict failure and growth in the ductile to brittle and the purely ductile region. In these regions where the structure is sufficiently yielded a one parameter description is no longer sufficient to describe the crack-tip conditions (cf. McClintock, 1971). The reason for this is that when the structure is sufficiently yielded, the triaxiality of the stress field will be geometry dependent.

To enable the derivation of correct mathematical and numerical models for predicting the behaviour of the ductile to brittle fracture mode it seems necessary to possess a good understanding of the micro mechanisms of the fracture process. A critical point seems to be how the stress and strain fields are changing in front of a growing crack and how this affects the probability for the tearing to change over to a cleavage process.

The  $J$ - $Q$  approach has been used to derive a micro mechanical model for ductile to brittle fracture by for instance O'Dowd and Shih (1991). Here  $J$  sets the size scale of high stresses and large deformations, while  $Q$  scales the near-tip stress distribution relative to a high triaxiality reference stress state, corresponding to a long crack in an infinitely large body. When large scale yielding prevails, the maximum principal stress will decrease because of loss of triaxiality in the stress field. According to this the probability for cleavage fracture will decrease relative to the small scale yielding situation as long as the crack tip is stationary. Therefore ductile tearing may occur before cleavage fracture. Varias and Shih

(1993) investigated the near tip fields of a steadily growing crack obeying a one-parameter scaling. Among other things they found that the hydrostatic stress increases with the crack growth, until a steady state solution is reached. Thus, there is competition between this effect and the decrease in the hydrostatic part of the stress field due to loss of constraint. O'Dowd *et al.* (1994) have used FE-analyses to investigate the influence of specimen geometry and transient growth on the stress and strain crack-tip fields. They found that the finite strain zone ahead of a growing crack was significantly smaller than the finite strain zone at the onset of growth and that the maximum principal stress increased with about 6%. It was also observed that the stress peak moved closer to the crack tip for the growing crack and that the blunting was minimal, so that the crack retains a rather sharp profile during growth.

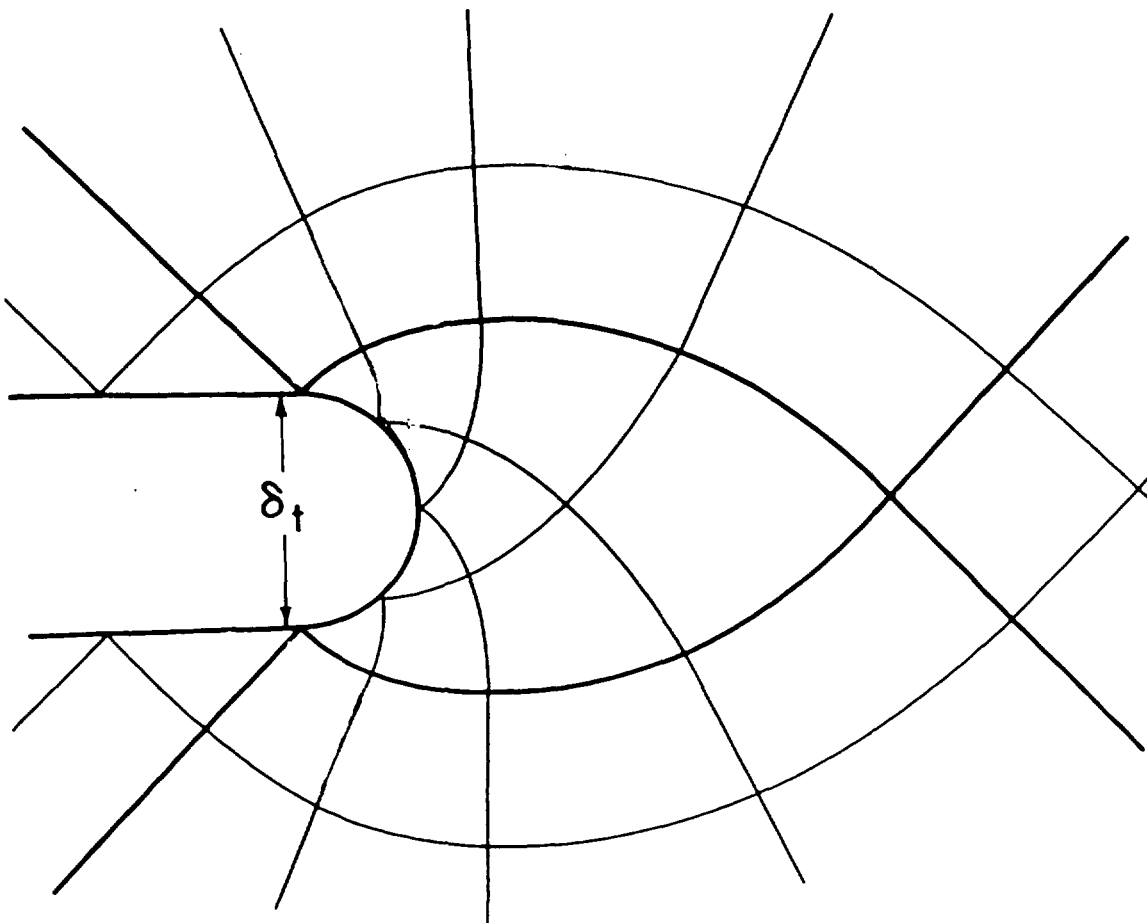


Figure 1: *Slip line field in front of a blunted crack, from Rice and Johnson (1970).*

Knott (1980) described the micromechanisms of ductile crack growth in metals. He distinguished between the two processes of internal necking and fast shear. It is a general agreement that a high hydrostatic stress field is necessary for voids to grow in the material even though they can be nucleated from dislocation pile-ups and by particle cracking caused by high plastic strains. In the internal necking process voids nucleate from parti-

cles poorly bonded to the matrix and at a distance of approximately 1.1 COD (Crack Tip Opening Displacement) from the crack tip. The void grows due to a high level of hydrostatic stress, and an instability point is reached when the crack tip joins with the void. In the fast shear case the crack links with nucleated voids along curved paths corresponding to the shear bands in front of a blunted notch (Fig. 1, from Rice and Johnson, 1970). The shear fracture mode develops easier in material with a low strain hardening and a high yield stress. When the crack grows by the mechanism of fast shear the crack will start to grow in the direction of maximum strain, *i.e.* at an angle of  $45^\circ$  with the prospective crack plane according to Anderson (1995). But due to global symmetry the crack must on a global scale remain in the original plane. The crack solves this by growing in a zig-zag pattern.

In this work a fairly systematic microscopic study on ductile crack growth in the A508B pressure vessel steel has been performed in order to qualitatively couple the newly developed theoretical results to direct observations. The main method of investigation was to subject fracture mechanics specimens (sub-sized three point bend specimens) to predetermined load levels corresponding to certain predetermined amounts of ductile crack extension. The specimens were then cut perpendicularly to the plane of the crack and the area in front of the crack was examined in a Scanning Electron Microscope (SEM). The object of these examinations was determine if the computational results discussed above could be correlated to crack extension characteristics and to study whether the mechanism of ductile growth was of the void growth type or of the fast shear mechanism. This is important for further numerical modelling of the process.

The material investigated has been subjected to two different heat treatments. The first one was the normal treatment performed by the manufacturer. A special additional heat treatment was also performed in order to raise the transition temperature to about  $60^\circ\text{C}$ , with the object to provide a more convenient testing situation. Charpy V tests were performed for the specially heat treated material to obtain the temperature dependence of the toughness. This was also studied by performing fracture toughness determination on the same type of specimens as were used for the microscopic study.

## Material

The material utilized in this investigation is the nuclear pressure vessel steel A508 with the composition shown in Table 1, which was used both in the as-delivered condition as well as after a modifying heat treatment. This heat treatment was performed in order to move the ductile-to-brittle transition of the original material to a temperature range where no cooling of the specimen would be necessary during testing. In the as-delivered condition, quenched and tempered, the transition covered the range  $-100 - 0^\circ\text{C}$  (Öberg, 1994, and Fig. 3). The possibility of moving the transition temperature to higher levels was dem-

onstrated in the Three Mile Island Vessel investigation project where the temperature history of the vessel could be inferred from among other things the transition behaviour of samples taken from different locations of the vessel (cf. Diercks and Neimark, 1994). The result of that project was that an increase in the austenitizing temperature results in an increase in the transition temperature.

C/%	Mn/%	Cr/%	Mo/%	Ni/%	Cu/%	S/%
0.18	0.92	0.46	0.57	0.79	0.11	0.003

Table 1: *Chemical composition of the material.*

In order to determine if a transition temperature suitable for the present purpose could be obtained, small Charpy V specimens were heat treated in a small furnace. Cooling of the specimens was done in air resulting in a cooling rate of approximately 50° C/min. For an austenitizing temperature of 1070° C during 15-20 minutes and no annealing afterwards a transition temperature near the target value was achieved. Next step was to realize this treatment in a piece large enough for cutting out large fracture mechanics specimens. The dimensions of the piece were 540 × 150 × 50 mm. The piece was heat treated at the same temperature, but the cooling had to be more efficient because of the larger mass. To get a cooling rate of approximately 50° C/min the piece was cooled with flowing argon gas. The microstructure for the heat treated steel can be seen in Fig. 2a.

The hardness was measured across a section in the middle of the piece, in order to check the homogeneity. The results are shown in Fig. 2b.

Fig. 3 shows three different Charpy V test series and  $J_{Ic}$  for subsized SEN(B) experiments as functions of temperature. The Charpy V results shown is for the original material, for the heat treated Charpy V specimens and for Charpy V specimens cut from the heat treated piece. An increase in the transition temperature of about 125° C can be seen. The difference between the material heat treated in the form of Charpy V specimens and the material heat treated as a large piece is small. The purpose of these tests was to check that the heat treatment procedure for the large piece would result in the desired transition behaviour.

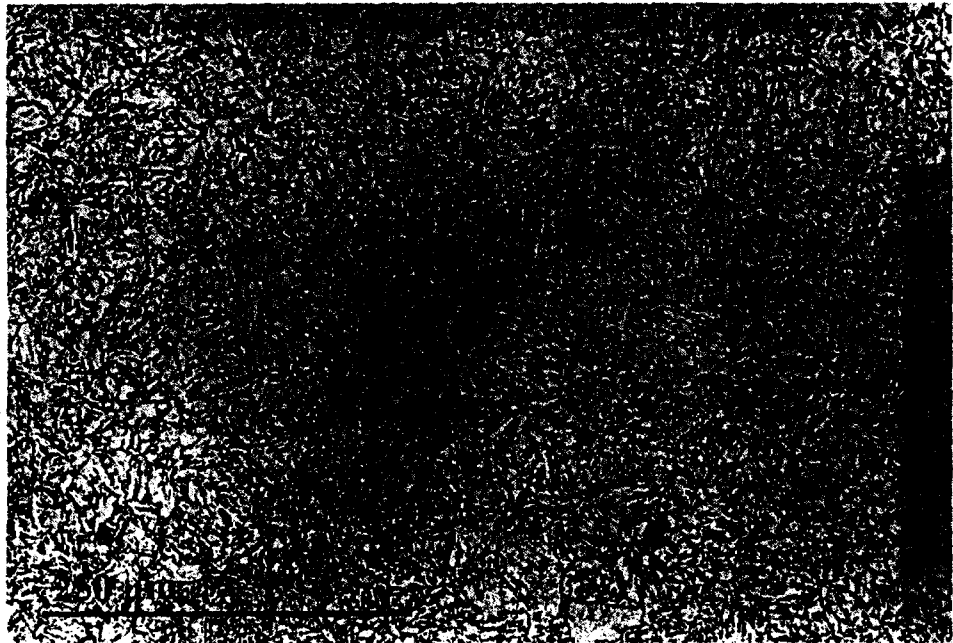


Figure 2a

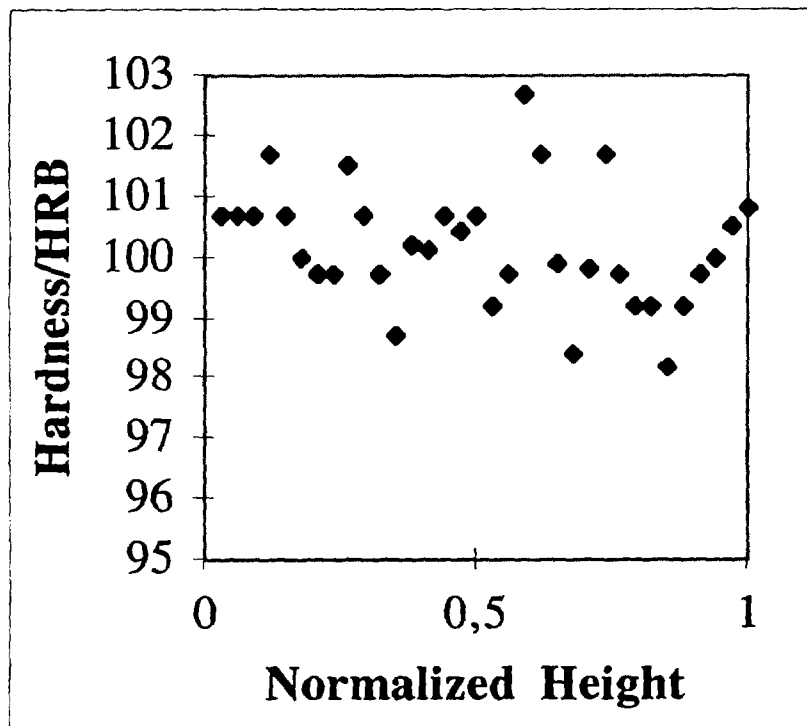
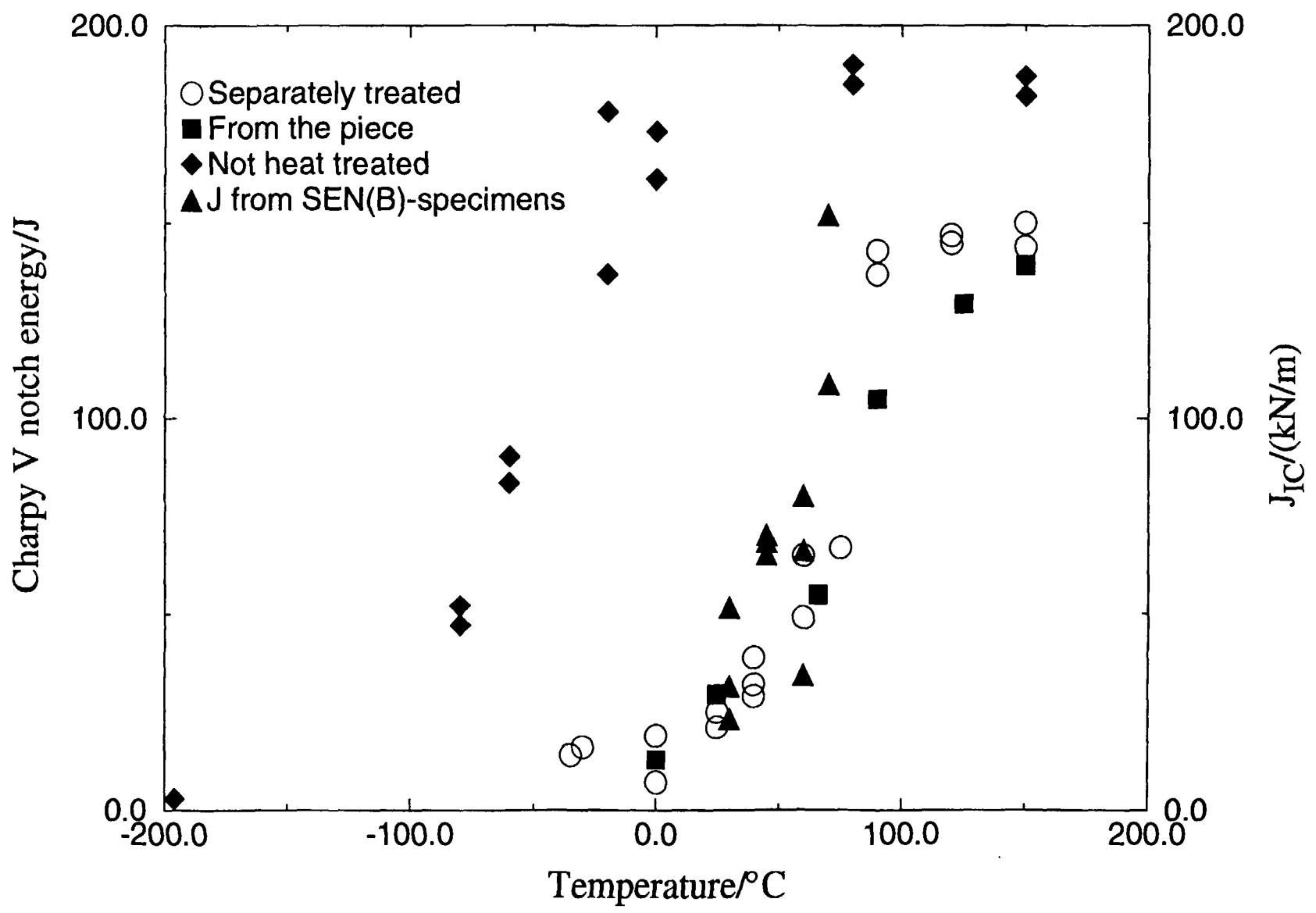


Figure 2b

Figure 2: Microstructure of heat treated material (Fig 2a) and hardness test results. (Fig. 2b).

Figure 3: Charpy V notch energy and  $J_{IC}$  for subsized SEN(B) experiments as functions of temperature.



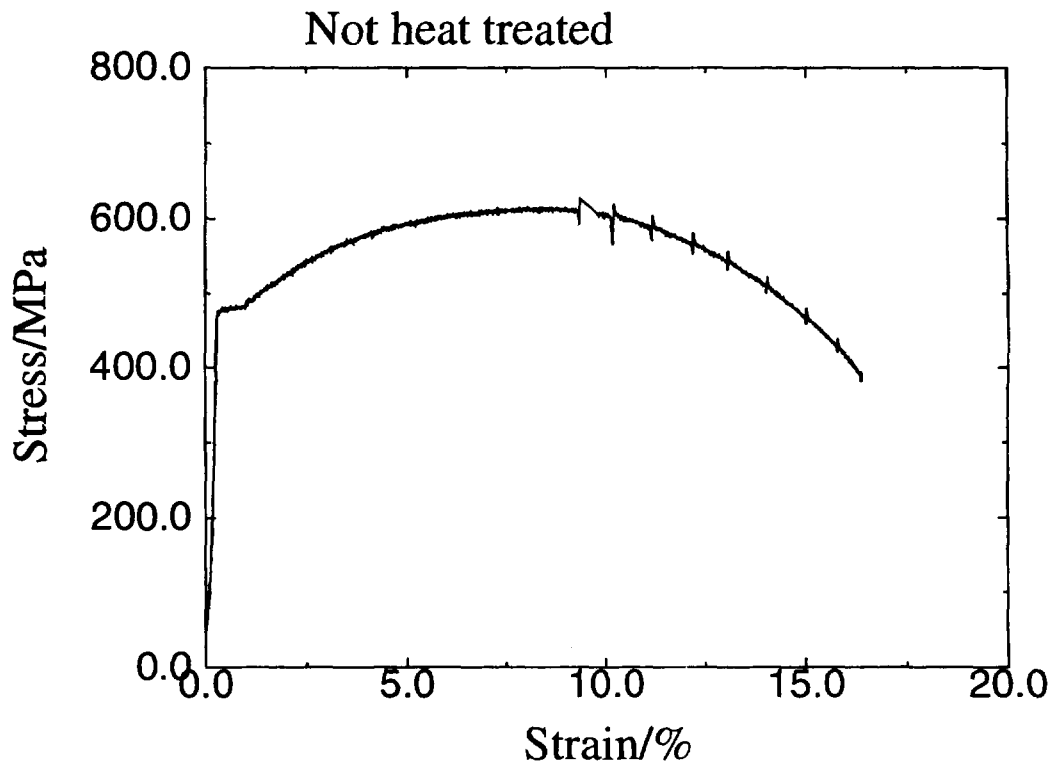
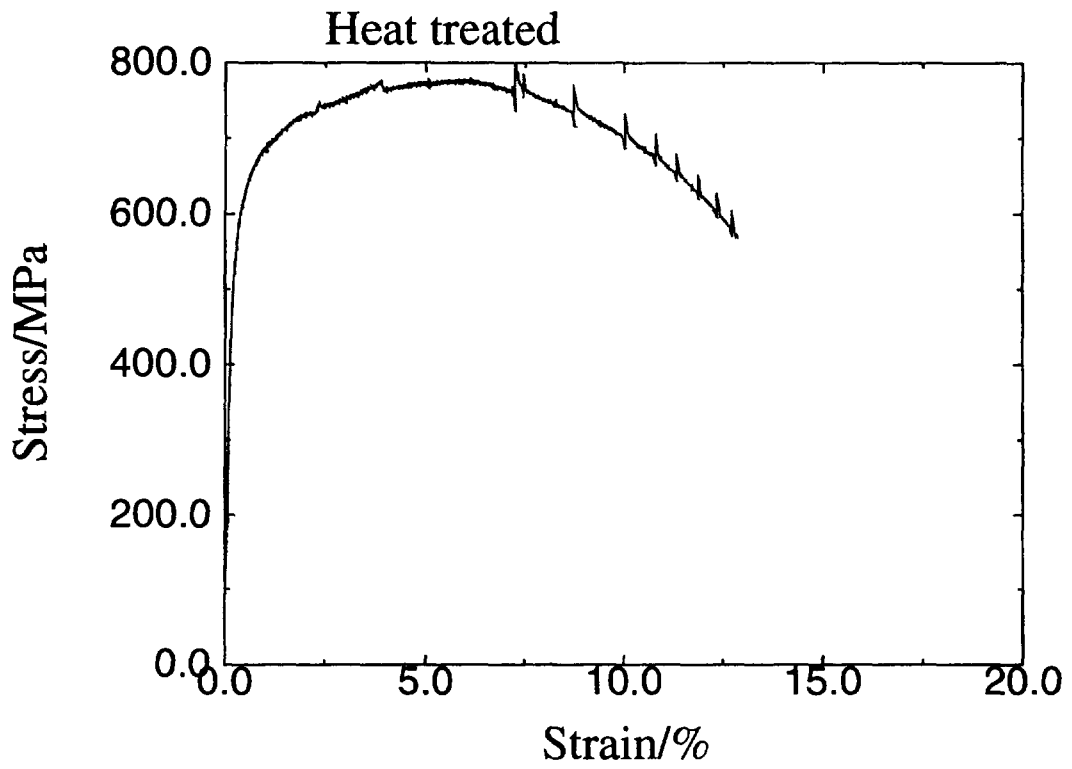


Figure 4: Tensile testing of original and modified material.

Tensile tests were performed at different temperatures for both the heat treated material from the piece and the original material. The tests were conventional low strain rate tests on round bars (5 mm), with a strain rate of 1.2%/min. The specimens were heated with an infrared heater. The strain was measured using two extensometers on each side of the tensile test specimen. Typical stress-strain curves are shown in Fig. 4. As can be seen in Fig. 4 the original material has a lower ultimate tensile strength (UTS) and larger total strain to failure than the heat treated material. The Lüders' strain in the original material has probably developed because the original material has been stored at ambient temperatures for 20 years. In the original material the yield stress  $\sigma_Y$  was taken as the lower yield stress ( $R_{e1}$ ) and in the heat treated material as  $R_{p0.2}$ . An equation of the type (1) was adjusted to the tensile data.

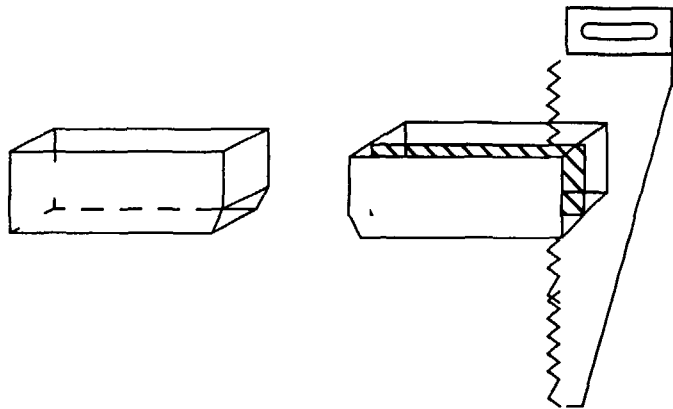
$$\frac{\varepsilon^P}{\varepsilon_Y} = \left( \frac{\sigma}{\sigma_Y} \right)^n - 1. \quad (1)$$

Here  $\varepsilon^P$  is the plastic strain and  $\varepsilon_Y$  the yield strain. The hardening exponent  $n$  was evaluated with the inclusion of post-necking data using the Bridgeman correction. Values of the different quantities are shown for different temperatures in Table 2.

Specimen no:	Heat treated	Test temperature/°C	E-modulus/GPa	$n$	$\sigma_Y, R_{p0.2}/\text{MPa}$	$R_m/\text{MPa}$
4594	no	0	210	8.3	567	802
4624	yes	60	213	8.3	560	766
4626	yes	60	212	8.3	563	777
4592	no	100	211	7.1	483	620
4593	no	100	209	7.1	477	626
4627	yes	100	214	7.7	542	799
4628	yes	100	210	8.3	567	802

Table 2: Conventional mechanical properties of the material.

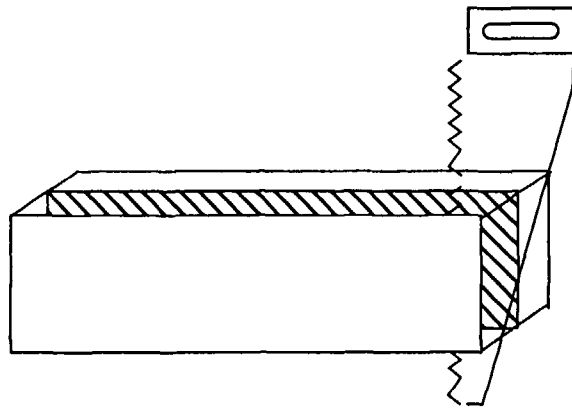
Figure 5: Subsize SEN(B) specimen and sketch of procedure for microscopic examination.



Cut and studied areas for specimens that failed by cleavage or pop-in.



**Areas studied with SEM**



Cut perpendicular to the crack plane for specimens with predetermined load levels.



**Area studied with SEM**

## Fracture mechanics testing

The fracture mechanics experimentation performed had two main objectives. First, the transition behaviour of the material was to be characterized in terms of fracture toughness and in particular the upper limit of the transition region was to be determined. Second, detailed microscopic examination of the fracture process from initiation to some amount of ductile growth was to be performed. To reach both these objectives, it was considered sufficient to use subsized SEN(B)-specimens.

### Specimen description

The specimens used were SEN(B)-specimens (Fig. 5) with the following dimensions: width  $W=10$  mm, span  $S=4W$ , thickness  $B=W$  and  $BN=0.8W$ . Here  $BN$  is the distance between the roots of the 45 degrees included side-grooves. The crack plane direction was the same in all specimens so that the crack plane was the same as the working direction. The specimens were precracked in the final heat treated condition before side grooving. The precracked specimens all had an initial crack size  $a$  of  $0.5W \mp 0.05W$ .

### Transition curve determination

As the objective was to characterize the transition behaviour and thus cleavage events are those of main interest, it was considered sufficient to determine the  $J$ -integral at the point of crack growth instability. This quantity is then termed the fracture toughness ( $J_{Ic}$ ). In practice the point of instability was defined as when the load versus displacement record of a specimen experienced a discontinuity corresponding to an increase of 1% or more in crack size.

The  $J$ -value was calculated as the sum of the elastic ( $J_e$ ) and plastic components ( $J_p$ ), according to the procedures in ASTM 813-89 (1990). During fracture toughness testing CMOD was measured using a clip gauge attached via grooves to the specimen. Slow stable crack growth was measured using the unloading compliance method. The specimens were heated with a infrared heater and the temperature was measured within  $\pm 1$  °C.

At each of the temperatures 30, 45, 60, 70, 80 and 100 °C, three specimens were tested. None of the specimens failed by cleavage or pop-in at 100 °C. At 80 °C one specimen failed by pop-in. In the temperature range 30-70 °C all specimens failed by cleavage or pop in. In the  $J_{Ic}$  versus temperature graph (Fig. 3) only those specimens that failed by cleavage or pop-in are shown. The results from the Charpy V testing is shown in the same figure to allow comparisons. It can be seen that the information about the transition behaviour by the Charpy tests is almost the same as by the fracture mechanics tests. The low-

er transition temperature seems to be around +10°C and the upper one around 80°C.

### Three point bend tests with predetermined load levels

In order to study how the crack tip blunts, crack growth initiates and continues in the ductile region a number of SEN(B)-specimens ( $W=10$  mm) were subjected to predetermined load levels, different for each specimen. Each load level corresponded approximately to a predetermined amount of growth. Both the specially heat treated material and the original material were studied. The specimens were after unloading from this level cut perpendicularly to the crack plane (Fig. 5) and the area in front of the crack was studied with SEM. The photographs provide a good picture of how the ductile growth is initiated and continued in this material. After the examination were two of the specimens successively polished, each time removing approximately 100  $\mu\text{m}$  of the surface and were thereafter examined again to study the three dimensional behaviour of the crack growth.

The test temperatures were chosen with the intention to give a ductile fracture behaviour. Test temperatures, number of specimens at each temperature and applied load levels are compiled in Table 3. Here the  $J$ -value is the area under the load-displacement curve which can be seen as a relative measure of the applied load level

Specimen no:	Temperature/°C	Heat treated	Applied load level $J/\text{kNm}$
4469	100	yes	75
4488	100	yes	90
4478	100	yes	125
4490	100	yes	175
4479	100	yes	225
4483	100	yes	400
4480	100	yes	500
4487	100	yes	595
4583	100	no	75
4585	100	no	125
4584	100	no	225
4582	100	no	400
4482	80	yes	225

Specimen no:	Temperature/°C	Heat treated	Applied load level J/kNm
4484	80	yes	400
4481	70	yes	300

Table 3: *Applied load levels and testing temperatures for subsized SEN(B)-specimens with predetermined load levels.*

## Microscopic examination

### Technical description of microscopic examination.

Two types of microscopic investigations were performed (Fig. 5). First, analyses of the fracture surfaces of the subsized SEN(B)-specimens that failed by cleavage or pop-in, and second, analyses of cross sections of those that showed a purely ductile fracture behaviour.

A JSM 840 Scanning Electron Microscope (SEM) was employed for the fracture surface analyses. Secondary electrons with an acceleration voltage of 10 kV and a large working distance (48 mm) were used. The samples for the cross section investigations were polished and about 85% of them etched with 4% nital. The remaining samples were not etched to see if this procedure could give more information. The cross section pictures were recorded digitally with a Zeiss 942 DMS, resolution 2048\*2048. Most of the pictures were taken with secondary electrons and an acceleration voltage of 10 kV. Other values of the acceleration voltage were tried. Some unetched samples were investigated with back scattered electrons. Short working distance and small probe current were used to get a high resolution.

### Results from the microscopic examination of the ductile crack growth

In this section we consider the pictures taken of the specimens tested at 100°C and with predetermined load levels. The photographic view is shown in Fig. 5. In Fig. 6 a sequence of pictures is shown which were taken from different specimens subjected to different load levels ( $J=75-595$  kN/m), corresponding to different amounts of ductile crack growth (0-2 mm). The sequence shows how the crack tip blunts, initiates and grows. The ductile growth can be seen to follow a zig-zag pattern.

The picture in Fig. 6a is taken from the mid section of a specimen where the applied load level ( $J=75$  kN/m) has caused blunting of the initially sharp crack. This specimen was successively polished and photographed, each time removing approximately 100  $\mu\text{m}$  of the specimen surface. The picture in Fig. 6a is characteristic for the different sections in the manner that micro cracks and voids seem to initiate in one of the “corners” of the blunted tip. In Fig. 6a a micro crack consisting of a cracked carbide package can be seen in the lower corner of the blunted tip. In the upper corner a void has nucleated around a slag particle. Along a grain boundary in the upper corner a void with fairly rectangular shape can also be seen. The small dark area in front of the blunted tip is just a shadow effect and not a crack. In the other sections of this specimens voids nucleated along grain boundaries were commonly seen. The crack in Fig. 6a is considered to be close to initiation. CTOD is at this load level of the order 50-60  $\mu\text{m}$ .

In Fig. 6b the applied load level ( $J=125$  kN/m) has forced the crack to grow further. This picture captures successfully the different mechanisms studied in different specimens. It is seen that the crack initiates in both the lower and the upper corner of the blunted tip but that it propagates along the upper path. The fracture path follows the slip lines in front of a blunted crack very well (compare with Fig. 1). The large void furthest from the crack tip is nucleated due to a cracked slag particle. It has been more difficult to decide the sources of the other large voids. These can emanate from slag particles but can also have been nucleated from smaller voids in the shear bands. From this picture and from pictures with higher magnification it can be seen that the crack shows a tendency to grow along the grain boundaries. In Fig. 7a the marked area in Fig. 6b is enlarged. In this area small voids have nucleated along straight lines emanating from the larger void. The distance between these voids is of the order of 1-5  $\mu\text{m}$ .

Fig. 7b shows the marked area in Fig. 6c. Here it can be seen how a couple of voids have nucleated along a path where the crack probably would have grown if a slightly higher load level were applied. The distance between these voids is of the order 10-30  $\mu\text{m}$ .

The specimen in Fig. 6d experienced a load level ( $J=595$  kN/m) corresponding to 2 mm growth. It can be seen that the crack growth still follows a zig-zag pattern, even after a relatively large amount of ductile growth.

In Fig. 7c the marked area in Fig. 6d is shown. In this picture the surface has dimples from relatively large voids connecting an even larger void, and the distance between these voids is of the order 20-30  $\mu\text{m}$ . Relatively large voids that nucleated from slag particles or cracked carbides can also be seen at a relatively large distance from the crack-tip.



Figure 6a



Figure 6c



Figure 6b

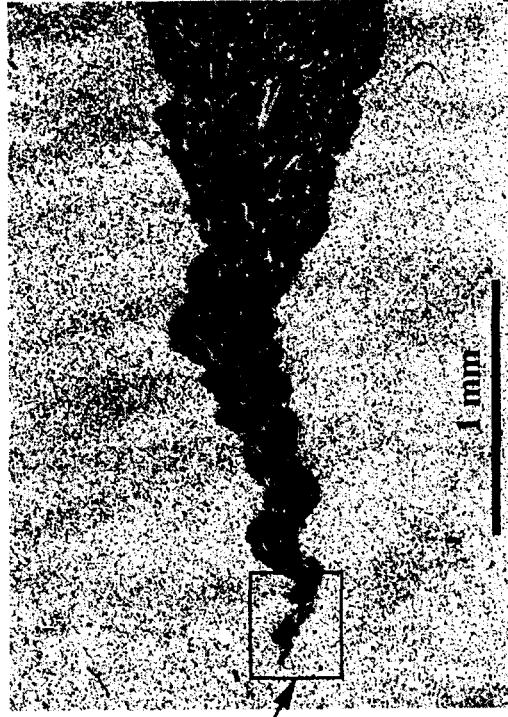


Figure 6d

Fig. 7a

Fig. 7c

Fig. 7b

Figure 6: Sequence of photographs taken perpendicularly to the crack plane at different stages of ductile crack growth.

Figure 7: Enlarged areas from photographs in Fig. 6.

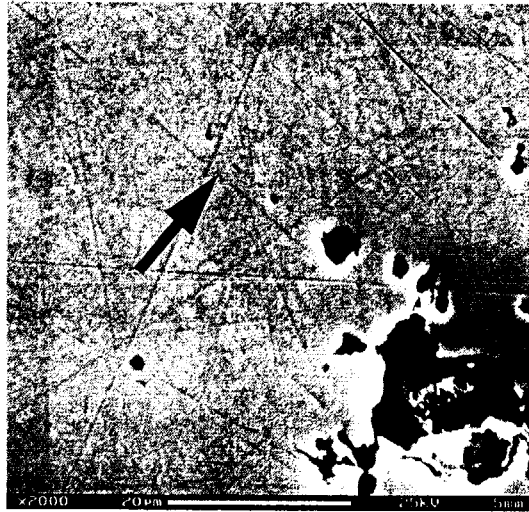


Figure 7a

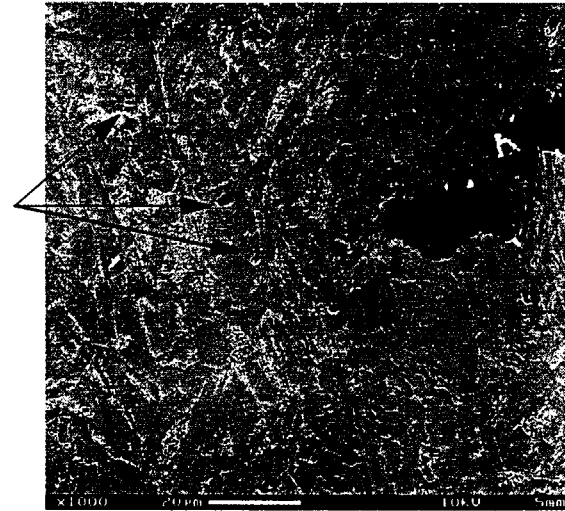


Figure 7b

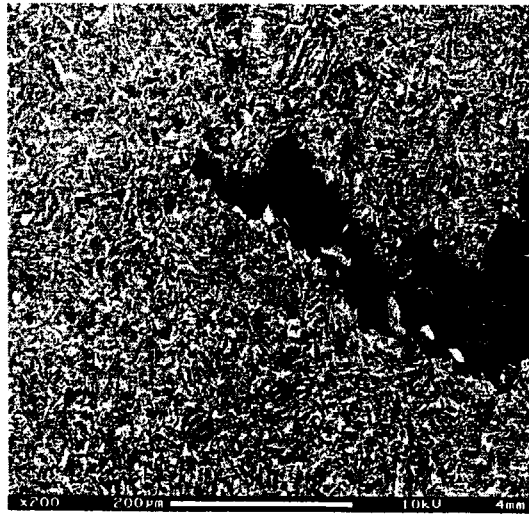


Figure 7c



Figure 7d

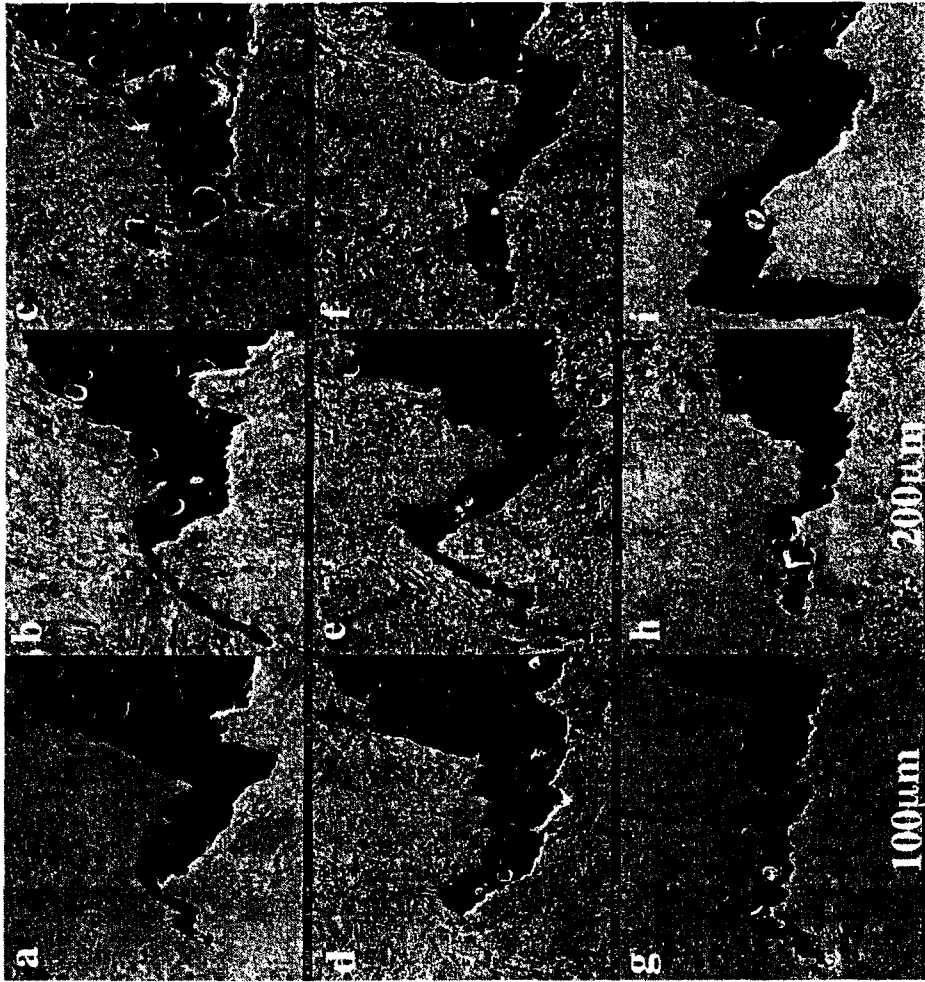


Figure 8a-i

Figure 8: *Photographs from different sections of a specimen subjected to a load level of  $J=225 \text{ kN/m}$ .*

In Fig. 7d a cracked slag particle can be seen in the upper right corner. The larger void below the cracked carbide shows under closer inspection dimples from smaller voids. In the lower part of the picture it is seen how voids and micro cracks nucleate from a boundary connecting four different grains and from cracked carbides inside the grains.

Fig. 8 shows a sequence of photographs from the same specimen ( $J=225$  kN/m). The first picture is from the mid-section and the following were taken after successively removing approximately 100  $\mu\text{m}$  of the specimen surface. Notice that the scale in picture 8 differs from the others which has the same scale as Fig. 8g. It can be noted that in this sequence which covers approximately 1 mm of the crack front, the zig-zag pattern seems to start in the downward direction. Notice also the rather big difference in crack shape along the front.

### **Discussion of the ductile crack growth and its micromechanisms**

The ductile crack growth seems to follow a zig-zag pattern, which is characteristic for some materials. It is especially materials with low strain hardening and high yield stress that exhibit this behaviour. This can be explained by the fact that the strain is at maximum at an angle of  $45^\circ$  with the prospective crack plane. It is a general agreement that voids can nucleate due to a high plastic strain. A material with low strain hardening will not be able to sustain so much further loading when increases in stresses and strains occur close to impurities or voids in the material. This will lead to that strain localization takes place (Knott, 1980). This often occurs in the maximum strain direction but due to global symmetry the crack must on a global scale remain in the original plane. As mentioned above the crack solves this by growing in a zig-zag pattern (Anderson, 1995). A material with higher strain hardening could sustain the higher stresses and start to deform plastically at another site without shear localization taking place. Thus in the present material shear deformation seems to be a critical feature in describing the ductile crack growth. The initial crack growth follows very well the slip lines in front of the blunted crack. This is of course only the case in the first step of the process, since the growth changes the slip line field.

In most of the cases studied above, the crack growth seems to start with a micro void nucleated from a cracked particle or carbide package alternatively by debonding between the matrix and inclusions. These voids grow together and join with the crack tip, along paths with localized shearing. The ligament between larger inclusions often appears as it has been sheared off. In some pictures micro cavities which are one to two orders of magnitude smaller are found within the bands. The cavities nucleated by small particles along the path of localized shear can play a crucial role in the process of linking the larger voids together by softening the material and enable the linking process to take place. The crack will tend to follow a slip line which connects the crack tip and the most favourable void.

The fracture process in which cavities formed around large inclusions are linked through bands of localized shearing has been studied before (cf. Rogers, 1960, and others). Faleskog and Shih (1996) used FE-analyses to investigate the effect of a bimodal distribution of smaller voids or loosely bounded small particles in the material. Their calculations shows how the larger voids enlarge with plastic straining and develop stress concentrations at nearby micro voids. At a critical stress level some micro voids will driven by the stored elastic energy start to grow rapidly. This will increase stresses at other micro voids which then begin to grow. This process goes on in cascades, until the entire ligament has failed by shearing. Here the plastic straining will play an important role since the plastic yielding decreases the tangent modulus which decreases the critical stress for micro void cavitation. The critical role of elasticity driving the micro void growth implies that small inclusions can affect the fracture resistance especially in high strength steels.

The model used by Faleskog and Shih (1997) corresponds on a micromechanical level best to the pure void growth and coalescence model. Even if the major fracture mechanism in our material is shear localisation, the final rupture process seems to be the connecting between larger voids through bands of smaller voids as described above. The process is thus the shear localised fracture but on a more local scale of the void and coalescence mechanism, with the different processes playing different roles at the crack growth. These observations give further justification for the model used Faleskog and Shih (1997) and it seems highly possible that a similar model could be used for the present material.

The sequence in Fig. 8 shows how the crack shape is changing along the crack front. From these pictures it can be concluded that even if the stress field as a whole can be described by a model including one or more parameters, the stress field can on a more local scale vary significantly.

It is often seen in the pictures that small voids nucleate along grain boundaries as well as inside grains. Voids nucleated along the grain boundaries and points where grain boundaries meet are possibly nucleated due to dislocation pile-ups, and those inside the grains possibly due to cracking of small particles or by debonding between the matrix and the particle. The sources that in the ductile fracture process nucleate voids can be the same as those that in a ductile-brittle or brittle fracture would induce the cleavage mechanism. The pictures that have been studied also suggest that it is usually only one to three larger voids that interact with each other and the crack tip at the same time, which is potentially valuable information when a FE-model for the growth is designed.

It was mentioned in the introduction that ductile crack growth often precedes cleavage and that the transition from a ductile to brittle mode could be due to changes in the stress field in front of the growing crack. Before examining the pictures the possibilities of observing changes in the micromechanisms of the ductile growth due to changes in the stress field

were considered. A transition from a more shear localized fracture mode to one more of the void growth and coalescence type was a possibility anticipated. Such a transition can not be seen in this material for the applied load levels. While studying the pictures it thus seems that the occurrence of smaller voids in the shear bands increases with distance from the crack-tip and also with the crack growth. To substantiate this statement a thorough study of more cuts should be done including a statistical investigation. The voids nucleated also seem to have a slightly more round shape with increasing distance from the crack tip. These effects are possibly due to an increase in the hydrostatic stress field with the crack growth and the fact that very close to a blunted crack-tip the triaxiality is rather low due to the free surface of the blunted tip.

### **Results from the microscopic examination of the ductile to brittle region**

Fracture surfaces from samples that during loading failed by cleavage or pop-in were investigated. The samples were taken from the determination of the fracture toughness transition curve (see section 3.2). Samples, tested at 100° C, showed a completely ductile fracture surface while samples, tested at 30° C, showed completely brittle fracture. Between those temperatures ductile tearing precedes the cleavage event. These specimens were examined by breaking the specimens cooled in nitrogen and afterwards study the fracture surfaces in the SEM. It proved to be rather difficult to localize the site of the cleavage initiation point in this material. Further investigation will be performed in this area. It is possible to compare the load levels at initiation with the load levels used in the study of the ductile crack growth. This gives a picture of the state of the crack at initiation.

### **Conclusions**

- The heat treatment that has been used was successful for the purpose of elevating the transition temperature with 125 ° C for this material.
- The crack growth initiates in one of the corners of the blunted crack tip.
- The mechanism of the ductile crack growth is of the localized shear type in which voids nucleated from slag particles or cracked carbides in front of the crack-tip join with the tip through bands of localized shearing. These bands coincide in the beginning of the growth with the slip lines in front of a blunted crack.
- The crack growth often extends along grain boundaries, where small voids nucleate and grow to become the new fracture surface.
- The distribution of particles that nucleates voids which contribute to the ductile fracture is at least bimodal and contains particles of vastly different sizes, each type con-

tributing to the fracture at different stages at the growth.

- The number of larger voids that interact with the crack-tip during growth is on a two dimensional cut one to three.
- Any substantial differences in the fracture process due to changes in the stress field could not be seen.

## References

Anderson, T., *Fracture Mechanics, Fundamentals and Applications*, CRC Press, Inc. 1995.

ASTM E 813-89 (1990), *Annual Book of ASTM Standards*, Vol. 03.01, American Society for Testing and Materials, Philadelphia, 1990

Diercks, O. R., and Neimark, L. A., in *Proc.of the Open Forum of the Three Mile Island reactor pressure vessel investigation project*, 20-22 October 1993, OECD, Paris, p. 97, 1994.

Faleskog, J., and Shih, C. F., Micromechanics of Coalescence-I. Synergistic effects of Elasticity, Plastic Yielding and Multi-Size-Scale Voids, to appear in *J. Mech. Phys. Solids*, 1997.

Knott, J. F., *Met. Sci.*, 14, p. 327, 1980.

McClintock, F. A., "Plasticity Aspects of Fracture", in H. Liebowitz (ed.), *Fracture: An Advanced treatise, Vol. III*, Academic Press, New York, p. 47,1971.

O'Dowd, N. P., and Shih, C. F., *J. Mech. Phys. Solids*, 39, p. 989, 1991.

O'Dowd, N. P., Shih C. F., and Dodds, Jr., R., in M. Kirk and A. Bakker (eds), *Constraint Effects in Fracture: Theory and Applications, ASTM STP 1244*, American Society For Testing and Materials, Philadelphia, 1994.

Rice, J. R., and Johnson, M. A., in M.F. Kaninnen, W.F. Adler, A.R. Rosenfield and R.I. Jaffee (eds), *Inelastic Behaviour of Solids* , McGraw Hill, p. 641, 1970.

Ritchie, R. O., Knott, J. F., and Rice, J. R., *J. Mech. Phys. Solids*, 21, p. 395, 1973.

Rogers, H. C., *Transactions of the Metallurgical Society of AIME*, 218, p. 498, 1960.

Varias, A. G., and Shih, C. F., *J. Mech. Phys. Solids*, 41, p. 835, 1993.

Wallin, K., Saario, T., and Törrönen, K., *Met. Sci.*, 18, p. 13, 1984.

Wallin, K., *Eng. Fract. Mech.*, 32, p. 449, 1989a.

Wallin, K., *Eng. Fract. Mech.*, 32, p. 523, 1989b

Wallin, K., in K. Salama, K. Ravi-Chandar, D.M.R. Taplin and P. Rama Rao (eds), *Ad-*

*vances in Fracture Research (Fracture 89), 7th International Conference on Fracture, 1:267, 1989c.*

Wallin, K., in J. G. Blauel and K. H. Schwalbe (eds), *Defect Assessment in Components-Fundamentals and Applications,ESIS/EGF9*, Mechanical Engineering Publications, London, 1991.

Öberg, H., *Impact testing, Influence of Orientation*. Internal report, Dept. of Solid Mechanics, KTH, 1994.



STATENS KÄRNKRAFTINSPEKTION  
Swedish Nuclear Power Inspectorate

---

**Postadress/Postal address**

SKI  
S-106 58 STOCKHOLM

**Telefon/Telephone**

Nat 08-698 84 00  
Int +46 8 698 84 00

**Telefax**

Nat 08-661 90 86  
Int +46 8 661 90 86

**Telex**

11961 SWEATOM S